Constructing tensegrity frameworks and related applications in multi-agent formation control

Yang, Qingkai

Chapter 6

Stress matrix-based formation scaling control

This chapter investigates the formation scaling control problem for multi-agent systems by mapping the formation into a universally rigid tensegrity framework with the underlying graph representing the agents and their interaction relationship. We first propose distributed formation scaling control laws by utilizing the stress of the universally rigid tensegrity framework. It is shown that global exponential convergence to the prescribed formation in $\mathbb{R}^d$ can be achieved by only controlling d pairs of agents whose position vectors span $\mathbb{R}^d$, under the assumption that each of the d pairs of agents has the knowledge of the desired formation size. Then by employing the technique of orthogonal projection, we design a new class of distributed control laws under which the agents are steered to form the desired formation under the relaxed assumption that only one pair of agents knows the scaling size; it is further proved that if the stress in the developed control law admits a generic universally rigid tensegrity framework, the equilibria correspond only to the translation and scaling of the given configuration among all the possible affine transformations. Finally, we propose a class of estimator-based control strategies, which can solve the formation scaling problem under the stricter condition that only one agent knows the prescribed size of the formation. Numerical simulations are carried out to validate the theoretical results.

6.1 Introduction

There has been a significant increase in the research on cooperative control of multi-agent systems. A fundamental task for cooperative control is formation control, which has found a wide range of applications, including networked mobile sensors performing ocean sampling tasks, a group of mobile robots enclosing a target, and unmanned aircrafts imaging in space [11, 73]. The main objective of distributed formation control is to design control laws using only local information to realize a given prescribed formation shape.

In general, the shape of a formation can be specified by various types of variables: absolute position, relative position (or displacement), distance, bearing

[138], and complex Laplacian [77]. In position-based control, each agent is informed of its absolute position and the desired position with respect to a global coordinate system, where agents can be controlled individually without any interaction with their neighbors. Therefore, network interaction among agents is not required but a global coordinate system for all agents is needed [91]. When the relative position becomes the sensed and controlled variable, the desired realizable formation can be achieved based on consensus algorithms using only measurements from local coordinate systems. However, the orientations of the local coordinate systems are required to be the same as that of a global coordinate system. In recent years, researchers have thoroughly studied the relative-position-based formation control from various aspects: linear and nonholonomic agent dynamics [79, 127]; undirected and directed switching interaction graphs [62, 92]; continuous- and discrete-time models [28, 130], to name a few.

In comparison, it is allowed in distance-based formation control that the sensed variable, i.e., relative position, can be measured in an arbitrary local coordinate system for each agent [91, 115]. However, using the gradient control protocols, only local stability is guaranteed for distance-based control systems under general graphs. In this scenario, rigidity graph theory has been shown to be an effective tool for analyzing the equilibrium formations up to translations and rotations. In [70], infinitesimal rigidity is shown to be a sufficient condition for locally asymptotically stabilizing an equilibrium formation under gradient control laws. To investigate global stability for triangular formations in the plane, it is shown in [14] that properly initialized formations can be controlled to exponentially converge to the desired formation with proper orientation. Note that to implement gradient control laws, relative positions are measured. The paper [15] proposes a stop-and-go cyclic strategy, which can stabilize a generically minimally rigid formation using only inter-agent distances. More recently, researchers have investigated the formation robustness issues, and have established formation movements in the presence of measurement mismatches [87, 116].

Investigating formation scaling is a growing major concern within formation control since the formation with varying size can dynamically adapt to changing environments in practice, such as obstacle avoidance for a group of vehicles. In [27], via a projection operator approach, two strategies are designed for the case when the scaling parameter is known to some of the agents. However, for the single-link method developed in [27], the monitoring graph needs to be chosen to contain all the vertices in the sensing graph. Later, the projection operator is also employed in [138], where bearing-based control frameworks are established. In addition, [54] addresses the formation scaling problem for both single- and double-integrator agent dynamics in the context of complex Laplacians.

In this chapter, we adopt a stress matrix-based approach to control a formation with the desired scaling, where the stress may contain negative values. It is worth

noting that most of the interacting weights in consensus-based protocols are positive. However, in some complex networks, e.g., social networks, the weights of the links cannot always be guaranteed to be positive. It is also shown in [129] that negative weights could contribute to faster convergence speed. Therefore, it is meaningful to incorporate negative weights in cooperative control. The stress matrix, defined in the same structure as a typical Laplacian matrix, is widely used to represent the stresses of edges and their connection relationships in a framework. Stress can be interpreted physically as the force per unit length, whose sign indicates the direction of the force. Hence, the stress matrix implicitly captures the features of a framework, e.g., rigidity, stability, and robustness [25]. Recently, a new type of formation pattern called affine formation has been investigated in [78], in which necessary and sufficient graphical conditions to achieve an affine formation are presented by employing the concept and properties of universal rigidity theory. It has also been revealed that an affine transformation of a given configuration is invariant to translation and scaling.

Motivated by these results, the goal of the current chapter is to first design distributed formation scaling control algorithms using the stress associated with a universally rigid tensegrity framework, such that the desired formation with predefined size in $\mathbb{R}^d$ is achieved. In the control algorithm, d pairs of agents whose position vectors span $\mathbb{R}^d$ are assumed to know the desired formation size, which renders the global exponential stability of the closed-loop system. Then to relax the condition that the chosen d pairs of the agents need to know the size, we propose orthogonal-projection-based control laws, where only *two* neighboring agents are required to be aware of the desired formation size. We show that the affine formation can be constrained to only translation and scaling even though only two of them have access to the desired size of the formation. Furthermore, under the more restrictive condition that only *one* agent knows the prescribed size, we design a class of estimator-based control laws, which successfully stabilize the agents to a predefined pattern from disordered initial formations. As a consequence, the feasibility of the proposed control law is highly improved in practice.

The rest of this chapter is organized as follows. Section 6.2 introduces the formation scaling control problem. In Section 6.3, we present basic stress matrix-based cooperative control laws for controlling formation scaling, followed by the stability analysis of the closed-loop system. Section 6.4 provides a new type of control laws by combining the stress and orthogonal projections. In Section 6.5, we introduce another type of estimator-based control strategies to further reduce the number of agents knowing the scaling parameter. Simulation results are presented in Section 6.6. Finally, we draw the conclusion in Section 6.7.

6.2 Problem formulation

Consider a group of $n \geqslant d+2$ mobile agents, each of which is modeled by single integrator dynamics

$$\dot{q}_i = u_i, \quad i = 1, \cdots, n, \tag{6.1}$$

where $q_i \in \mathbb{R}^d$ is the position of agent i and $u_i \in \mathbb{R}^d$ is the control input. Given a generic universally rigid tensegrity framework $(\mathcal{G}, q^*)$ with an equilibrium stress ω, the objective of formation scaling is, by using the stress ω, to design distributed control laws $u_i(q_i^* - q_j^*, q_i - q_j), j \in \mathcal{N}_i$, such that

$$\lim_{t\to\infty} (q_i(t) - q_j(t)) = \kappa(q_i^* - q_j^*), \forall (i,j) \in \mathcal{E}, \tag{6.2}$$

where κ is a positive constant indicating the size of the formation. Here, by mapping the multi-agent system to the universally rigid tensegrity framework, we assigned each edge of the formation with a weight (or stress), which can be either positive or negative.

Remark 6.1. The formation scaling problem becomes trivial if each agent knows the scaling parameter κ. However, in this chapter, we show the formation scaling can still be achieved using the proposed algorithms even only a small number of agents knows κ.

6.3 Formation scaling control using the stress matrix

In this section, we consider the formation scaling control problem, in which the formation can expand or shrink according to the parameter κ defined in (6.2). Distributed control laws are proposed by employing the stress of a universally rigid tensegrity framework.

Before moving on, we select d pairs of nodes in the given universally rigid tensegrity framework $(\mathcal{G}, q^*)$, such that the dimension of the convex hull of the selected nodes is d. Denote the set of edges corresponding to the d pairs of chosen nodes as $\mathcal{E}_l$. All the nodes involved in $\mathcal{E}_l$ are assembled in the node set $\mathcal{V}_l = \{1, \cdots, n_l\}$, and the set of the remaining nodes in $\mathcal{V}$ is denoted by $\mathcal{V}_f = \{n_l + 1, \cdots, n\}$. Here, the d pairs of nodes are chosen such that the resultant subgraph $\mathcal{G}_l(\mathcal{V}_l, \mathcal{E}_l)$ is connected. It is worth noting that the chosen d pairs of nodes can involve less than $2d$ nodes, due to the common endpoint shared by distinct edges. Fig. 6.1 shows an example of the setup for the subgraph $\mathcal{G}_l(\mathcal{V}_l, \mathcal{E}_l)$, where the dashed lines and solid lines represent the cables and struts, respectively.

(a) A tensegrity framework $(\mathcal{G}, q^*)$ in R^2.

(b) $\mathcal{E}_l = \{(1,2),(2,3)\}$, $\mathcal{V}_l = \{1,2,3\}$.

Figure 6.1: *An example of setting* $\mathcal{G}_l(\mathcal{V}_l, \mathcal{E}_l)$.

Then the control input for each agent i is designed as

$$u_i = -\sum_{(i,j)\in\mathcal{E}} \omega_{ij}(q_i - q_j) - \sum_{(i,j)\in\mathcal{E}_l} a_{ij}\left[(q_i - q_j) - \kappa(q_i^* - q_j^*)\right], \tag{6.3}$$

where ω_{ij} is the stress of member (i,j). It can be seen that the control input includes two parts:

$$u_i^F = -\sum_{(i,j)\in\mathcal{E}} \omega_{ij}(q_i - q_j), \tag{6.4}$$

and

$$u_i^S = -\sum_{(i,j)\in\mathcal{E}_l} a_{ij}\left[(q_i - q_j) - \kappa(q_i^* - q_j^*)\right], \tag{6.5}$$

where the internal force u_i^F generated from the virtual tensegrity framework is used to stabilize the formation shape, and the input u_i^S is to realize formation scaling. Equivalently, the control input (6.3) can be written as

$$u_i = \begin{cases} u_i^F + u_i^S, & \text{if } i \in \mathcal{V}_l, \\ u_i^F, & \text{if } i \in \mathcal{V}_f. \end{cases}$$

One of the main results concerning the formation scaling is presented as follows.

Theorem 6.2. *For system* (6.1)*, by employing the virtual tensegrity-framework-based control law* (6.3) *for each agent, the target formation with the prescribed size is globally exponentially stabilized.*

Proof. The control input u_i^F in (6.3) can be written in the compact form as

$$u^F = -(\Omega \otimes I_d)\bar{q}, \tag{6.6}$$

where $\bar{q} = [q_1^T, \cdots, q_n^T]^T \in \mathbb{R}^{dn}$ and $u^F = \left[(u_1^F)^T, \cdots, (u_n^F)^T\right]^T$ are the vector form of q_i and u_i^F, respectively. Similarly, consider the scaling control part of (6.3),

i.e., u_i^S, which can be written in the vector form as

$$u^S = -(L_s \otimes I_d)\tilde{q}, \tag{6.7}$$

where u^S is the concatenated form of u_i^S, and $\tilde{q} = [\tilde{q}_1^T, \cdots, \tilde{q}_n^T]^T \in \mathbb{R}^{dn}$, with $\tilde{q}_i \in \mathbb{R}^d$ being defined by

$$\tilde{q}_i = q_i - \kappa q_i^*. \tag{6.8}$$

The matrix L_s is given by

$$L_s = \begin{bmatrix} L_l & \mathbf{0}_{n_l \times (n-n_l)} \\ \mathbf{0}_{(n-n_l)\times n_l} & \mathbf{0}_{(n-n_l)\times(n-n_l)} \end{bmatrix}, \tag{6.9}$$

where L_l is the Laplacian matrix associated with the agents in the set $\mathcal{N}_l$, defined by

$$[L_l]_{ij} = \begin{cases} \sum\limits_{j\in\mathcal{N}_i} a_{ij}, & i = j, \\ -a_{ij}, & i \neq j. \end{cases}$$

By combining (6.6) and (6.7), it follows

$$u = -\left((\Omega + L_s) \otimes I_d\right)\tilde{q}, \tag{6.10}$$

where we have used the equilibrium stress condition that $(\Omega \otimes I_d)\bar{q}^* = \mathbf{0}$, and $\bar{q}^*$ is defined as $\bar{q}^* = \left[(q_1^*)^T, \cdots, (q_n^*)^T\right]^T$. Then the dynamics of $\tilde{q}$ is given by

$$\dot{\tilde{q}} = -\left((\Omega + L_s) \otimes I_d\right)\tilde{q} \triangleq -\bar{\Omega}\tilde{q}. \tag{6.11}$$

Note that the stress matrix Ω is positive semi-definite, so is L_s. Therefore, the matrix $\tilde{A}$ is positive semi-definite. Hence, the equilibrium of the closed-loop system (6.11) is globally stable. Furthermore, the equilibrium points of system (6.11), denoted by q^e, satisfy

$$\dot{\tilde{q}}^e = -\left((\Omega + L_s) \otimes I_d\right)\tilde{q}^e \triangleq -\bar{\Omega}\tilde{q}^e = \mathbf{0}_{nd\times 1},$$

where $\tilde{q}^e$ is the stacked vector of $\tilde{q}_i^e = q_i^e - \kappa q_i^*, i = 1, \cdots, n$. It follows from Lemma 2.17 that

$$\tilde{q}^e \in \mathrm{null}(\Omega \otimes I_d), \quad \text{and} \quad \tilde{q}^e \in \mathrm{null}(L_s \otimes I_d). \tag{6.12}$$

Therefore, we have

$$\left[u_1^F, \cdots, u_n^F\right] = -\left(\sum_{(1,j)\in\mathcal{E}} \omega_{1j}(q_1^e - q_j^e), \cdots, \sum_{(n,j)\in\mathcal{E}} \omega_{nj}(q_n^e - q_j^e)\right) = \mathbf{0}, \tag{6.13}$$

and similarly,

$$\left[u_1^S, \cdots, u_n^S\right] = -(q^e - \kappa q^*)L_s = \mathbf{0}_{d\times n}. \tag{6.14}$$

Equivalently, we consider the reduced form of (6.14) as follows

$$\left[u_1^S, \cdots, u_{n_l}^S\right] = -(q_s^e - \kappa q_s^*)L_l = \mathbf{0}_{d\times n_l}, \tag{6.15}$$

where $q_s^e = [q_1^e, \cdots, q_{n_l}^e] \in \mathbb{R}^{d\times n_l}$, $n_l > d$, and $q_s^* = [q_1^*, \cdots, q_{n_l}^*]$.

Combining (2.5) and (6.13), we know q^e is the affine transformation of q^* with respect to Ω, i.e.,

$$q_i^e = Mq_i^* + b, \quad i = 1, \cdots, n, \tag{6.16}$$

where $M \in \mathbb{R}^{d\times d}$ and $b \in \mathbb{R}^d$. Substituting (6.16) into (6.15), yields

$$\left[(M - \kappa I_d)q_1^* + b, \cdots, (M - \kappa I_d)q_{n_l}^* + b\right] L_l = \mathbf{0}_{d\times n_l}. \tag{6.17}$$

Note that the Laplacian matrix L_l satisfies

$$\mathrm{null}(L_l) = \mathrm{span}(\mathbf{1}_{n_l}). \tag{6.18}$$

Therefore, it follows from (6.17) and (6.18) that

$$\mathrm{span}\left[(M - \kappa I_d)q_1^* + b, \cdots, (M - \kappa I_d)q_{n_l}^* + b\right] = \mathrm{span}(\mathbf{1}_{n_l}),$$

i.e.,

$$\mathrm{span}[(M - \kappa I_d)q_s^* + (b \otimes \mathbf{1}_{n_l}^T)] = \mathrm{span}(\mathbf{1}_{n_l}). \tag{6.19}$$

In view of $n_l > d$, to make (6.19) hold, it requires

$$(M - \kappa I_d)q_s^* = [\xi, \cdots, \xi],$$

where $\xi \in \mathbb{R}^d$ is any arbitrary real vector. Then we obtain

$$(M - \kappa I_d)(q_i^* - q_j^*) = \mathbf{0}, \quad i, j \in \mathcal{V}_l. \tag{6.20}$$

By recalling that the dimension of the convex hull of $(q_i^* - q_j^*), i, j \in \mathcal{V}_l$, is d, it follows from (6.20) that $M = \kappa I_d$. Then, we can draw the conclusion that formation scaling is achieved.

Note that

$$\mathrm{null}(\Omega) = \mathrm{span}\left((q^*)^T, \mathbf{1}_n\right). \tag{6.21}$$

Since q converge to κq^*, only the freedom of translation is left for the stabilized formation, which results from the basis $\mathbf{1}_n$ in the null space of Ω. Note that

$$\mathrm{span}(\mathbf{1}_n) \in \mathrm{null}(L_s).$$

Consequently, again from Lemma 2.17, we have

$$\text{null}\left((\Omega + L_s)\right) = \text{span}(\mathbf{1}_n). \tag{6.22}$$

Now, we show the convergence is achieved globally exponentially and derive the guaranteed exponential rate.

Define the formation centroid by

$$q_c = \frac{1}{n}\sum_{i=1}^{n} q_i = \frac{1}{n}(\mathbf{1}_n \otimes I_d)^T \bar{q}.$$

Then the dynamics of the centroid satisfy

$$\dot{q}_c = \frac{1}{n}(\mathbf{1}_n \otimes I_d)^T \dot{\tilde{q}} = \frac{1}{n}(\mathbf{1}_n \otimes I_d)^T \left((\Omega + L_s) \otimes I_d\right) \tilde{q} = 0,$$

which implies that the centroid of the formation keeps static. Following the same line of the proof in [118, Theorem 3], we construct an orthogonal matrix $S \in \mathbb{R}^{dn\times dn}$ as

$$S = \begin{pmatrix} \frac{1}{\sqrt{n}}(\mathbf{1}_n \otimes I_d)^T \\ S_r \end{pmatrix},$$

where $S_r \in \mathbb{R}^{d(n-1)\times dn}$. Then consider the coordinate transformation

$$p = S\tilde{q} = \begin{pmatrix} p_c \\ p_r \end{pmatrix}, \tag{6.23}$$

where $p_c = \frac{1}{\sqrt{n}}(\mathbf{1}_n \otimes I_d)^T(\bar{q} - \kappa\bar{q}^*) = \sqrt{n}q_c - \kappa\sqrt{n}q_c^*$, with q_c^* defined by $q_c^* = 1/n\sum_{i=1}^{n} q_i^*$. From (6.23), one has

$$\tilde{q} = S^{-1}p = S^T p. \tag{6.24}$$

Taking the derivative of both sides of (6.23), we have

$$\dot{p} = S\dot{\tilde{q}} = -S\bar{\Omega}\tilde{q} = -S\bar{\Omega}S^T p.$$

Equivalently,

$$\begin{aligned}\begin{bmatrix} \dot{p}_c \\ \dot{p}_r \end{bmatrix} &= -S\bar{\Omega}S^T \begin{bmatrix} p_c \\ p_r \end{bmatrix} \\ &= -\begin{bmatrix} \frac{1}{\sqrt{n}}(\mathbf{1}_n \otimes I_d)^T \\ S_r \end{bmatrix} \bar{\Omega} \begin{bmatrix} \frac{1}{\sqrt{n}}(\mathbf{1}_n \otimes I_d)^T \\ S_r \end{bmatrix}^T \begin{bmatrix} p_c \\ p_r \end{bmatrix}\end{aligned}$$

$$= \begin{bmatrix} \mathbf{0}_{d\times d} & \mathbf{0}_{d\times d(n-1)} \\ \mathbf{0}_{d(n-1)\times d} & S_r\tilde{A}S_r^T \end{bmatrix} \begin{bmatrix} p_c \\ p_r \end{bmatrix}.$$

Consequently, the transformed system dynamics become

$$\begin{cases} \dot{p}_c = \mathbf{0} \\ \dot{p}_r = -S_r\bar{\Omega}S_r^T p_r \end{cases}. \tag{6.25}$$

In view of (6.22), we know the matrix $S_r\bar{\Omega}S_r^T$ is positive definite. Therefore, the state p_r will globally exponentially converges to the equilibrium $p_r = \mathbf{0}$. Recalling (6.24) with orthogonal matrix S and the fact that p_c keeps constant, we draw the conclusion that $\tilde{q}$ globally exponentially converges to zero, which implies q converges to κq^* globally exponentially from (6.8). This implies that the formation scaling is achieved in the sense of globally exponential stability. In addition, it can be seen from (6.25) that the convergence rate depends on the eigenvalues of matrix $\bar{\Omega}$, or equivalently, matrices Ω and L_s. □

Remark 6.3. From (6.21), it is clear that if one only uses the control law u_i^F in (6.4), then there is no constraint for the size of the formation. Therefore, the idea of designing the u_i^S in (6.5) is to reduce the dimension of the null space of Ω, namely, to restrict the null space of $(\Omega \otimes I_d)$ to $span(\mathbf{1}_n \otimes I_d)$. To achieve this goal, at least d pairs of agents are required to construct the sub-Laplacian matrix L_l in (6.9).

6.4 Formation scaling control via the stress matrix and orthogonal projections

In Section 6.3, we have shown that the formation scaling problem can be solved using the proposed control law (6.3) if d pairs of agents have accesses to the formation scaling parameter κ. Aiming to further reduce the number of the agents knowing κ, in this section, we present a new class of distributed control laws by utilizing the orthogonal projections.

To facilitate the design of control laws, we choose $d+1$ members in $(\mathcal{G}, q^*)$, automatically yielding $d+1$ pairs of nodes corresponding to the chosen $d+1$ members, such that the dimension of the convex hull spanned by any d pairs of the chosen nodes is d. The subgraph associated with those $d+1$ pairs of agents is denoted by $\mathcal{G}_l(\mathcal{V}_l, \mathcal{E}_l)$, with $|\mathcal{V}_l| = n_l$, $|\mathcal{E}_l| = d+1$. Here, the nodes are also properly chosen to make subgraph $\mathcal{G}_l(\mathcal{V}_l, \mathcal{E}_l)$ connected. Correspondingly, we have $\mathcal{V}_f$ and $\mathcal{E}_f$, such that $\mathcal{V}_l \cup \mathcal{V}_f = \mathcal{V}$ and $\mathcal{E}_l \cup \mathcal{E}_f = \mathcal{E}$. As illustrated before, there must be fewer

than $2(d+1)$ nodes involved in the chosen $d+1$ members due to the connectivity constraint of the subgraph $\mathcal{G}_l(\mathcal{V}_l, \mathcal{E}_l)$. Fig. 6.2 shows an example of determining the sub-graph $\mathcal{G}_l(\mathcal{V}_l, \mathcal{E}_l)$, where the dashed lines and solid lines represent cables and struts, respectively.

(a) A tensegrity framework $(\mathcal{G}, q^*)$ in $\mathbb{R}^2$.

(b) $\mathcal{V}_l = \{1,2,3\}$,$\mathcal{E}_l = \{(1,2),(2,3),(1,3)\}$.

Figure 6.2: *An example of determining* $\mathcal{G}_l(\mathcal{V}_l, \mathcal{E}_l)$.[1]

Then the incidence matrix H can be partitioned as

$$H = \left(\begin{array}{c:c} H_{ll} & H_{lf} \\ \hdashline H_{fl} & H_{ff} \end{array}\right), \tag{6.26}$$

where $H_{ll} \in \mathbb{R}^{n_l \times (d+1)}$, $H_{lf} \in \mathbb{R}^{n_l \times (m-d-1)}$, $H_{fl} \in \mathbb{R}^{(n-n_l)\times(d+1)}$, and $H_{ff} \in \mathbb{R}^{(n-n_l)\times(m-d-1)}$. Furthermore, from the definition of the sets $\mathcal{V}_l$ and $\mathcal{E}_l$, we know that no vertex in $\mathcal{V}_f$ is adjacent to the edges in $\mathcal{E}_l$, which implies $H_{fl} = \mathbf{0}$.

Suppose none of the agents has the knowledge of κ. However, the information of κ is implicitly contained in one specific edge. Without loss of generality, we assume this edge is adjacent to agents 1 and 2. This means $\kappa(q_1^* - q_2^*)$ is known by agents 1 and 2 as a whole piece of information. For other edges in the edge set $\mathcal{E}_l$, only the information of $q_i^* - q_j^*, (i,j) \in \mathcal{E}_l \backslash (1,2)$, is available to their adjacent agents.

Define an auxiliary variable $z = [z_1^T, \cdots, z_m^T]^T \in \mathbb{R}^{md}$ as follows

$$z = (H^T \otimes I_d)q,$$

where H is the incidence matrix, and $z_\iota = q_i - q_j, \iota = 1, \cdots, m$, with agents i and j being the head and tail of the ιth edge, respectively. To be consistent, we assume the specific edge connecting agents 1 and 2 is labeled as the 1st edge. Therefore, it follows $z_1 = q_1 - q_2$. Analogously, we have

$$z^* = (H^T \otimes I_d)q^*.$$

[1]Fig. 6.2 differs from Fig. 6.1 in the edge set $\mathcal{E}_l$ of the subgraph (b), where there is one more edge $(1,3)$ in Fig. 6.2(b) compared with Fig. 6.1(b).

The projection of z_ι along z_ι^* is given by

$$\kappa_\iota = \frac{1}{\|z_\iota^*\|^2}(z_\iota^*)^T z_\iota, \quad \iota = 2, \cdots, d+1. \tag{6.27}$$

The projection method is also employed in [27, 138], where the projection operator (6.27) is used to 'estimate' the scaling parameter [27] and to realize the bearing-based control [138].

The control inputs for agents 1 and 2 are designed as

$$u_1 = -\sum_{(1,j)\in\mathcal{E}} \omega_{1j}(q_1 - q_j) - h_{11}(z_1 - \kappa z_1^*) - \sum_{\iota=2}^{d+1} h_{1\iota}(z_\iota - \kappa_\iota z_\iota^*), \tag{6.28}$$

and

$$u_2 = -\sum_{(2,j)\in\mathcal{E}} \omega_{2j}(q_2 - q_j) - h_{21}(z_1 - \kappa z_1^*) - \sum_{\iota=2}^{d+1} h_{2\iota}(z_\iota - \kappa_\iota z_\iota^*). \tag{6.29}$$

where ω_{ij} is the stress associated with member (i,j). It is worth noting that even though κz_1^* is contained in the control laws (6.28) and (6.29), agents 1 and 2 have no knowledge of the value of κ, since κz_1^* is transmitted as a whole piece of information. The reason that the desired information of edge 1 is written as κz_1^* is to facilitate the stability analysis. For the rest of the agents, their control inputs $u_i, i = 3, \cdots, n$, are given by

$$u_i = -\sum_{(i,j)\in\mathcal{E}} \omega_{ij}(q_i - q_j) - \sum_{\iota=2}^{d+1} h_{i\iota}(z_\iota - \kappa_\iota z_\iota^*). \tag{6.30}$$

Similar to (6.3), the proposed control input for each agent consists of two parts: the internal force $-\sum_{(i,j)\in\mathcal{E}} \omega_{ij}(q_i - q_j)$ generated from the virtual tensegrity framework used to drive the whole group of agents to the affine space of the configuration q^*, and the rest used to fix the size of the formation. To implement the proposed control inputs (6.28)-(6.30) in practice, agents 1 and 2 can be arbitrarily chosen among the $d+1$ pairs of agents. The proposed control input has a similar part as the control laws proposed in [27, 138], while we introduce the negative weight that can model the antagonistic interactions between neighbor agents. Furthermore, using the stress matrix makes it possible that only a few number of agents are required to have the common knowledge of the global coordinate system, which will greatly broaden the applicability of the proposed control laws in practice. In addition, even though the conditions to achieve affine formations in the context of graph theory are presented in [78], no control law on formation

(scaling) control has been given.

Then we are ready to present another main result as follows.

Theorem 6.4. *Suppose the given generic framework $(\mathcal{G}, q^*)$ is universally rigid with an equilibrium stress ω. Then for a group of agents modeled by* (6.1)*, the formation scaling control task* (6.2) *can be achieved globally using the proposed distributed control laws* (6.28)- (6.30).

Proof. Since $\kappa_\iota z_\iota^* = z_\iota^* \kappa_\iota$, for κ_ι defined in (6.27) is a scalar, we have

$$z_\iota - \kappa_\iota z_\iota^* = \left(I_d - \frac{(z_\iota^*)(z_\iota^*)^T}{\|z_\iota^*\|^2} \right) z_\iota. \tag{6.31}$$

The vector corresponding to the right-hand side of (6.31) is in the direction of $(z_\iota^*)^\perp$. The (orthogonal) projection is to project vector z_ι to the orthogonal complement of z_ι^*. We denote the orthogonal projection operator as $Proj_\iota \triangleq I_d - \frac{(z_\iota^*)(z_\iota^*)^T}{\|z_\iota^*\|^2}$, $\iota = 2, \cdots, d+1$. Since κz_1^* is known to agents 1 and 2, to keep consistent with the notations, we denote $Proj_1 \triangleq I_d$.

Then the control laws (6.28)-(6.30) can be integrated as

$$\begin{aligned} u_i = &- \sum_{(i,j)\in\mathcal{E}} \omega_{ij}(q_i - q_j) - \sum_{\iota=1}^{d+1} h_{i\iota} Proj_\iota(z_\iota - \kappa z_\iota^*), \\ &i = 1, \cdots, n, \end{aligned} \tag{6.32}$$

where we have used the fact that

$$Proj_\iota(\kappa z_\iota^*) = \mathbf{0}_d, \quad \forall \kappa \in R, \quad \iota = 2, \cdots, d+1.$$

The compact form of (6.32) is in the form

$$u = -(\Omega \otimes I_d)q - (\bar{H}_{ll} \otimes I_d)\bar{P}_l(z - \kappa z^*), \tag{6.33}$$

where

$$\bar{H}_{ll} = \left(\begin{array}{c|c} H_{ll} & \mathbf{0}_{n_l \times (m-d-1)} \\ \hline \mathbf{0}_{(n-n_l)\times(d+1)} & \mathbf{0}_{(n-n_l)\times(m-d-1)} \end{array} \right),$$

and

$$\bar{P}_l = \mathrm{diag}(Proj_1, \cdots, Proj_{d+1}, \mathbf{0}_d, \cdots, \mathbf{0}_d).$$

Note that

$$(\Omega \otimes I_d)(\kappa q^*) = \kappa(\Omega \otimes I_d)q^* = \mathbf{0}. \tag{6.34}$$

Substituting (6.34) into (6.33), we have

$$u = -(\Omega \otimes I_d)(q - \kappa q^*) - (\bar{H}_{ll} \otimes I_d)\bar{P}_l(z - \kappa z^*). \tag{6.35}$$

In light of the fact that $z = (H^T \otimes I_d)q$, (6.35) can be rewritten as

$$u = -(\Omega \otimes I_d)(q - \kappa q^*) - (\bar{H}_{ll} \otimes I_d)\bar{P}_l(H^T \otimes I_d)(q - \kappa q^*). \tag{6.36}$$

Recalling that $H_{fl} = \mathbf{0}$ in (6.26), one has

$$\begin{aligned} &(\bar{H}_{ll} \otimes I_d)\bar{P}_l(H^T \otimes I_d) \\ &= \left(\begin{array}{c:c} H_{ll} \otimes I_d & \mathbf{0} \\ \hdashline \mathbf{0} & \mathbf{0} \end{array}\right) \left(\begin{array}{c:c} P_l & \mathbf{0} \\ \hdashline \mathbf{0} & \mathbf{0} \end{array}\right) \left(\begin{array}{c:c} H_{ll}^T \otimes I_d & \mathbf{0} \\ \hdashline H_{lf}^T \otimes I_d & H_{ff}^T \otimes I_d \end{array}\right) \\ &= \left(\begin{array}{c:c} (H_{ll} \otimes I_d)P_l(H_{ll}^T \otimes I_d) & \mathbf{0} \\ \hdashline \mathbf{0} & \mathbf{0} \end{array}\right) \triangleq \Psi, \end{aligned} \tag{6.37}$$

where $P_l = \mathrm{diag}(Proj_1, \cdots, Proj_{d+1})$. Combining (6.36) and (6.37), we have

$$\dot{q} - \kappa\dot{q}^* = -\left((\Omega \otimes I_d) + \Psi\right)(q - \kappa q^*). \tag{6.38}$$

It can be checked that the eigenvalues of the matrix $(z_\iota^*)(z_\iota^*)^T/\|z_\iota^*\|^2$ are $\{0, \cdots, 0, 1\}$, where the algebraic multiplicity of eigenvalue 0 is $d-1$. Hence, the nonzero eigenvalue of the projection operator $Proj_\iota$ is 1 with the algebraic multiplicity $d-1$. This implies that the matrix $(H_{ll} \otimes I_d)P_l(H_{ll}^T \otimes I_d)$ is positive semi-definite, and so is the matrix Ψ. Note that for a universally rigid framework $(\mathcal{G}, q^*)$, its stress matrix Ω is positive semi-definite. Therefore, the equilibrium of the closed-loop system (6.38) is globally stable. In addition, the equilibrium points of system (6.38), denoted by q^e, satisfy

$$-\left((\Omega \otimes I_d) + \Psi\right)(q^e - \kappa q^*) = \mathbf{0}.$$

In view of Lemma 2.17, we have

$$\begin{cases} (\Omega \otimes I_d)(q^e - \kappa q^*) = \mathbf{0}, & (6.39) \\ \Psi(q^e - \kappa q^*) = \mathbf{0}. & (6.40) \end{cases}$$

Note that for a generic and universally rigid tensegrity framework $(\mathcal{G}, q^*)$, it follows from Lemma 2.9 that its corresponding stress matrix Ω is positive semi-definite with rank $n - d - 1$. Moreover, for the stress ω in equilibrium with q^*, in

view of the definition of Ω, we know

$$\text{null}(\Omega) = \text{span}\left(\begin{bmatrix} q_{11}^* \\ q_{21}^* \\ \vdots \\ q_{n1}^* \end{bmatrix} \begin{bmatrix} q_{12}^* \\ q_{22}^* \\ \vdots \\ q_{n2}^* \end{bmatrix} \cdots \begin{bmatrix} q_{1d}^* \\ q_{2d}^* \\ \vdots \\ q_{nd}^* \end{bmatrix} \begin{bmatrix} 1 \\ 1 \\ \vdots \\ 1 \end{bmatrix}\right).$$

Then, it follows that q^e is an affine transformation of q^*, i.e.,

$$q_i^e = Mq_i^* + b, \tag{6.41}$$

where $M \in \mathbb{R}^{d\times d}$ and $b \in \mathbb{R}^d$. Substituting (6.41) into (6.40), we get

$$\Psi\left((I_n \otimes M)q^* + (\mathbf{1}_n \otimes b) - \kappa q^*\right) = \mathbf{0}. \tag{6.42}$$

In view of the structure of Ψ in (6.37), (6.42) can be reduced to

$$(D_{ll} \otimes I_d)P_l(D_{ll}^T \otimes I_d)\left[(I_{n_l} \otimes M)q_l^* + (\mathbf{1}_{n_l} \otimes b) - \kappa q_l^*\right] = \mathbf{0}. \tag{6.43}$$

Note that

$$(D_{ll}^T \otimes I_d)(\mathbf{1}_{n_l} \otimes b) = D_{ll}^T\mathbf{1}_{n_l} \otimes b = \mathbf{0}. \tag{6.44}$$

Then (6.43) can be equivalently written as

$$(D_{ll} \otimes I_d)P_l(D_{ll}^T \otimes I_d)\left[(I_{n_l} \otimes M)q_l^* - \kappa q_l^*\right] = \mathbf{0}. \tag{6.45}$$

To determine the value of matrix M, we write (6.45) in the componentwise form

$$\sum_{\iota=1}^{d+1} \xi_\iota = \mathbf{0},$$

where edge ι is assumed to be adjacent to vertices i and j, and ξ_ι is given by

$$\xi_\iota = \begin{pmatrix} \cdots & \cdots & \cdots & \cdots & \cdots \\ \cdots & h_{i\iota}^2 Proj_\iota & \cdots & h_{i\iota}h_{j\iota}Proj_\iota & \cdots \\ \vdots & \vdots & \ddots & \vdots & \vdots \\ \cdots & h_{j\iota}h_{i\iota}Proj_\iota & \cdots & h_{j\iota}^2 Proj_\iota & \cdots \\ \cdots & \cdots & \cdots & \cdots & \cdots \end{pmatrix} \begin{pmatrix} \cdots \\ (M-\kappa I_d)q_i^* \\ \vdots \\ (M-\kappa I_d)q_j^* \\ \cdots \end{pmatrix}. \tag{6.46}$$

Noting that $h_{i\iota}h_{j\iota} = -1$, for each edge ι, we have

$$Proj_\iota(M-\kappa I_d)(q_i^* - q_j^*) = \mathbf{0},$$

i.e.,

$$Proj_\iota(M-\kappa I_d)z_\iota^*=\mathbf{0}.$$

Next, we will prove by contradiction that $M=\kappa I_d$. Assume $M\neq\kappa I_d$. Recalling that $Proj_1=I_d$, and that $Proj_\iota(\alpha z_\iota^*)=\mathbf{0}$, we get

$$\begin{cases}(M-\kappa I_d)z_1^*=0,\\(M-\kappa I_d)z_2^*=\alpha_2 z_2^*,\\\qquad\vdots\\(M-\kappa I_d)z_{d+1}^*=\alpha_{d+1}z_{d+1}^*,\end{cases}\tag{6.47}$$

where $\alpha_\iota\neq 0, \iota=2,\cdots,d+1$.

Since the dimension of the convex hull spanned by any d pairs of the agents in the set $\mathcal{V}_l$ is d, there exist $\beta_i, i=2,\cdots,d+1$, such that

$$z_1^*=\beta_2 z_2^*+\cdots+\beta_{d+1}z_{d+1}^*,\tag{6.48}$$

where at least one of the coefficients β_i is nonzero. Then multiplying $(M-\kappa I_d)$ on both sides of (6.48), we obtain

$$(M-\kappa I_d)z_1^*=(M-\kappa I_d)(\beta_2 z_2^*+\cdots+\beta_{d+1}z_{d+1}^*)=\mathbf{0}.\tag{6.49}$$

Combining (6.47) and (6.49), we have

$$\begin{aligned}&(M-\kappa I_d)(\beta_2 z_2^*+\cdots+\beta_{d+1}z_{d+1}^*)\\=&\beta_2(M-\kappa I_d)z_2^*+\cdots+\beta_{d+1}(M-\kappa I_d)z_{d+1}^*\\=&\alpha_2\beta_2 z_2^*+\cdots+\alpha_{d+1}\beta_{d+1}z_{d+1}^*\\=&\mathbf{0},\end{aligned}\tag{6.50}$$

where at least one of $\alpha_\iota\beta_\iota, \iota=2,\cdots,d+1$, is nonzero.

Considering again that any d pairs of agents in $\mathcal{V}_l$ linearly span $\mathbb{R}^d$, it is obvious that vectors $z_2^*,\cdots,z_d^*$, and z_{d+1}^* are linearly independent. This implies that $\mathbf{0}_d$ is the unique solution of $\gamma=[\gamma_1,\cdots,\gamma_d]^T$ to the following equation

$$\gamma_1 z_2^*+\cdots+\gamma_d z_{d+1}^*=\mathbf{0},$$

which contradicts (6.50). Therefore, the assumption $M\neq\kappa I_d$ does not hold. In other words, $M=\kappa I_d$. Then, from (6.41) we know

$$q_i^e=\kappa q_i^*+b,\quad i=1,\cdots,n_l.$$

Consequently, it follows

$$z_\iota = \kappa z_\iota^*, \quad \iota = 1, \cdots, d+1.$$

Then one can draw the conclusion from Lemma 2.16 that formation scaling for the whole group of agents is achieved. This completes the proof. □

6.5 Estimation-based formation scaling control

In this section, we further extend the results in Section 6.4 by assuming only one agent knows the desired formation size, i.e., the scaling parameter κ. With the intention to drive the agents to form the prescribed formation pattern with fixed scaling, we design a new type of distributed estimator-based control laws.

It has been shown in Section 6.3 that the formation can be scaled to the prescribed size if d pairs of agents with the associated connected subgraph $\mathcal{G}_l(\mathcal{V}_l, \mathcal{E}_l)$ knows κ. Following the same principle of constructing the subgraph $\mathcal{G}_l(\mathcal{V}_l, \mathcal{E}_l)$, we know there must exist a path $(1, 2, \cdots, n_l)$ through relabeling the agents due to the bidirectional property of an undirected graph. Without loss of generality, we assume only agent 1 knows the scaling parameter κ among the $|\mathcal{V}_l|$ agents.

Assumption 6.5. For any given q_i^*, $i = 2, \cdots, n$, there holds

$$|\mathcal{N}_{i-1}^l|(q_{i-1}^* - q_i^*) + \sum_{j \in \mathcal{N}_{i-1}^l \cap \mathcal{N}_i^l} (q_i^* - q_j^*) \neq \mathbf{0}_d. \tag{6.51}$$

Remark 6.6. In the working space $\mathbb{R}^d$, $d \in \{2, 3\}$, if the subgraph $\mathcal{G}_l(\mathcal{V}_l, \mathcal{E}_l)$ is chosen as a complete graph, then condition (6.51) reduces to the principle constructing the subgraph, namely, the dimension of the convex hull spanned by the nodes of $\mathcal{V}_l$ is d. To reveal the implicit connections, we take $d = 2$ as an example. Note that (6.51) can be equivalently written as

$$(q_1^* - q_2^*) + (q_1^* - q_3^*) \neq \mathbf{0},$$

and

$$(q_2^* - q_3^*) + (q_2^* - q_1^*) \neq \mathbf{0},$$

which implies q_1^*, q_2^* and q_3^* are linearly independent. So the three nodes linearly span $\mathbb{R}^2$.

With these background knowledge, the control input for agent 1 is the same as

(6.3), given by

$$u_1 = -\sum_{j\in\mathcal{N}_1}\omega_{1j}(q_1-q_j) - \sum_{j\in\mathcal{N}_1^l} a_{1j}\left((q_1-q_j)-\kappa(q_1^*-q_j^*)\right), \tag{6.52}$$

where $\mathcal{N}_1^l$ denotes the set of neighbor agents of agent 1 in the subgraph $(\mathcal{E}_l,\mathcal{V}_l)$. For the rest, we introduce the following estimation-based control protocols

$$\begin{aligned} u_i = &-\sum_{j\in\mathcal{N}_i}\omega_{ij}(q_i-q_j) \\ &-\sum_{j\in\mathcal{N}_i^l} a_{ij}\left((q_i-q_j)-\hat{\kappa}_i(q_i^*-q_j^*)\right), \quad i=2,\cdots,n, \end{aligned} \tag{6.53}$$

where $\hat{\kappa}_i$ is the estimation of κ by agent i. As illustrated in Section 6.3, the first part of the control input is used to achieve the affine formations associated with the stress ω, and the second part aims to fix the formation size from the affine formations. It can be observed from (6.52)-(6.53) that only agent 1 knows the desired size of the formation, and the others employ the estimation variable $\hat{\kappa}_i, i=2,\cdots,n_l$, in their control inputs. We propose the following estimators for agent 2

$$\begin{cases} \dot{\theta}_2 = -\Lambda_2\xi_2^T\zeta_2 \\ \hat{\kappa}_2 = -\theta_2 - \Lambda_2\xi_2^T(q_2-q_1) \end{cases}, \tag{6.54}$$

and for agent $i, i=3,\cdots,n_l$,

$$\begin{cases} \dot{\theta}_i = -\Lambda_i\xi_i^T\zeta_i \\ \hat{\kappa}_i = \hat{\kappa}_{i-1} - \theta_i - \Lambda_i\xi_i^T(q_i-q_{i-1}) \end{cases}, \tag{6.55}$$

where θ_i is an intermediate variable, and Λ_i is a positive scalar. The variables ξ_i and ζ_i are respectively given by

$$\xi_i = |\mathcal{N}_{i-1}^l|(q_{i-1}^*-q_i^*) + \sum_{j\in\mathcal{N}_{i-1}^l\cap\mathcal{N}_i^l}(q_i^*-q_j^*), \tag{6.56}$$

and

$$\begin{aligned} \zeta_i = &\hat{\kappa}_i\left(|\mathcal{N}_{i-1}^l|+1\right)(q_{i-1}^*-q_i^*) - \sum_{j\in\mathcal{N}_i}\omega_{ij}(q_i-q_j) \\ &-\sum_{j\in\mathcal{N}_i^l} a_{ij}(q_i-q_j) + \sum_{k\in\mathcal{N}_{i-1}}\omega_{(i-1)k}(q_{i-1}-q_k) \\ &+\sum_{k\in\mathcal{N}_{i-1}^l} a_{(i-1)k}(q_{i-1}-q_k), \quad i=2,\cdots,n_l. \end{aligned} \tag{6.57}$$

Remark 6.7. As can be seen from (6.54) and (6.55), two-hop information is required to implement the relative-position-based estimator. Similar estimation problem was also addressed in [82] to estimate an unknown rotation parameter, in which the estimator is designed under the complete graph. In addition, it stated that constructing estimator using only relative position information under a general connected graph is an open problem.

Proposition 6.8. *Consider the estimator* (6.54) *and* (6.55) *for agent* $i, i = 2, \cdots, n_l$. *Then, we have* $lim_{t\to\infty}\hat{\kappa}_i = \kappa$.

Proof. First considering the control inputs for the first two agents, we obtain their dynamics from (6.52) and (6.53) as

$$\begin{aligned}\dot{q}_2 - \dot{q}_1 =& -\sum_{j\in\mathcal{N}_2}\omega_{2j}(q_2 - q_j) + \sum_{k\in\mathcal{N}_1}\omega_{1k}(q_1 - q_k)\\ &- \sum_{j\in\mathcal{N}_2^l} a_{2j}\left((q_2 - q_j) - \hat{\kappa}_2(q_2^* - q_j^*)\right)\\ &+ \sum_{k\in\mathcal{N}_1^l} a_{1k}\big((q_1 - q_k) - \kappa(q_1^* - q_k^*)\big).\end{aligned} \tag{6.58}$$

Define the estimation error for agent 2 by

$$\tilde{\kappa}_2 = \hat{\kappa}_2 - \kappa, \tag{6.59}$$

and denote the quantity associated with κ and $\hat{\kappa}$ in (6.58) by q_{2r}^*, i.e.,

$$q_{2r}^* \triangleq \sum_{j\in\mathcal{N}_2^l} a_{2j}\hat{\kappa}_2(q_2^* - q_j^*) - \sum_{k\in\mathcal{N}_1^l} a_{1k}\kappa(q_1^* - q_k^*). \tag{6.60}$$

By invoking the fact that $q_1^* - q_k^* = q_1^* - q_2^* + (q_2^* - q_k^*)$, we have

$$\begin{aligned}q_{2r}^* =& \sum_{j\in\mathcal{N}_2^l} a_{2j}\hat{\kappa}_2(q_2^* - q_j^*) - \sum_{k\in\mathcal{N}_1^l} a_{1k}\kappa(q_2^* - q_k^*)\\ &- \sum_{k\in\mathcal{N}_1^l} a_{1k}\kappa(q_1^* - q_2^*)\\ =& \sum_{j\in\mathcal{N}_1^l\cap\mathcal{N}_2^l}(\hat{\kappa}_2 - \kappa)(q_2^* - q_j^*) + a_{21}\hat{\kappa}_2(q_2^* - q_1^*)\\ &- \sum_{k\in\mathcal{N}_1^l} a_{1k}\kappa(q_1^* - q_2^*) + \sum_{k\in\mathcal{N}_1^l} a_{1k}\hat{\kappa}_2(q_1^* - q_2^*)\\ &- \sum_{k\in\mathcal{N}_1^l} a_{1k}\hat{\kappa}_2(q_1^* - q_2^*)\end{aligned}$$

$$\begin{aligned} &= \tilde{\kappa}_2 \sum_{j\in\mathcal{N}_1^l\cap\mathcal{N}_2^l}(q_2^*-q_j^*) + \tilde{\kappa}_2|\mathcal{N}_1^l|(q_1^*-q_2^*) \\ &\quad + \hat{\kappa}_2(|\mathcal{N}_1^l|+1)(q_2^*-q_1^*). \end{aligned} \tag{6.61}$$

Substituting (6.61) into (6.58), we get

$$\dot{q}_2-\dot{q}_1 = \zeta_2 + \mathcal{N}_1^l|(q_1^*-q_2^*) + \sum_{j\in\mathcal{N}_1^l\cap\mathcal{N}_2^l}(q_2^*-q_j^*), \tag{6.62}$$

where ξ_2 and ζ_2 are defined in (6.56) and (6.57). By differentiating $\hat{\kappa}_2$ in (6.54), and replacing $\dot{q}_2-\dot{q}_1$ with (6.62), it follows

$$\dot{\tilde{\kappa}}_2 = -\tilde{\kappa}_2\Lambda_2\|\mathcal{N}_1^l|(q_1^*-q_2^*) + \sum_{j\in\mathcal{N}_1^l\cap\mathcal{N}_2^l}(q_2^*-q_j^*)\|^2. \tag{6.63}$$

Recall that the scaling parameter is constant, there holds $\dot{\kappa}=0$. Hence, it is straightforward to have

$$\dot{\tilde{\kappa}}_2 = \dot{\hat{\kappa}}_2 = -\tilde{\kappa}_2\Lambda_2\|\mathcal{N}_1^l|(q_1^*-q_2^*) + \sum_{j\in\mathcal{N}_1^l\cap\mathcal{N}_2^l}(q_2^*-q_j^*)\|^2. \tag{6.64}$$

Therefore, it is easy to know $\tilde{\kappa}_2$ converges to zero exponentially under Assumption 6.5, namely, $\lim_{t\to\infty}\hat{\kappa}_2(t)=\kappa$.

Analogously, define the estimation error for agent $i, i=3,\cdots,n_l$ by

$$\tilde{\kappa}_i = \hat{\kappa}_i - \hat{\kappa}_{i-1}. \tag{6.65}$$

Similar to the calculations for agent 2, we get

$$\dot{\tilde{\kappa}}_i = -\tilde{\kappa}_i\Lambda_i\|\mathcal{N}_{i-1}^l|(q_{i-1}^*-q_i^*) + \sum_{j\in\mathcal{N}_{i-1}^l\cap\mathcal{N}_i^l}(q_i^*-q_j^*)\|^2 \tag{6.66}$$

In light of Assumption 6.5, we know $\lim_{t\to\infty}\tilde{\kappa}_i(t)=0$, which implies $\lim_{t\to\infty}\hat{\kappa}_i(t) = \hat{\kappa}_{i-1}(t)$, $i=3,\cdots,n_l$. Since $\lim_{t\to\infty}\hat{\kappa}_2=\kappa$, we can conclude that $\lim_{t\to\infty}\hat{\kappa}_{n_l} = \cdots=\hat{\kappa}_2=\kappa$. This completes the proof. □

Theorem 6.9. *Suppose the given generic framework $(\mathcal{G},q^*)$ is universally rigid with an equilibrium stress ω. Under Assumption 6.5, for a group of agents modeled by* (6.1)*, the formation scaling control problem can be solved in the sense of global stability using the proposed estimation-based control laws* (6.52) *and* (6.53).

Proof. Note that (6.53) can be written as

$$\begin{aligned} u_i = &- \sum_{j\in\mathcal{N}_i} \omega_{ij}(q_i - q_j) - \sum_{j\in\mathcal{N}_i^l} a_{ij}\left((q_i - q_j) - \kappa(q_i^* - q_j^*)\right), \\ &+ (\hat{\kappa}_i - \kappa) \sum_{j\in\mathcal{N}_i^l} a_{ij}(q_i^* - q_j^*), \quad i = 2, \cdots, n. \end{aligned} \tag{6.67}$$

Recalling (6.10), the compact form of (6.67) is given by

$$\dot{\tilde{q}} = ((\Omega + \mathcal{L}_s) \otimes I_d)\, \tilde{q} + \tilde{K}(L_s \otimes I_d) q^*, \tag{6.68}$$

where $\tilde{K}$ is a diagonal matrix defined by $\tilde{K} \triangleq \mathrm{diag}(()\hat{\kappa}_1 - \kappa, \cdots, \hat{\kappa}_{n_l} - \kappa)$. If follows from Theorem 6.2 that the autonomous part of system (6.68) is globally stable. In view of the fact that q^* is fixed and $\tilde{K}$ globally converge to zero from Proposition 6.8 , by invoking the input-to-state stability theorem [68], we can conclude that

$$\lim_{t\to\infty} (q_i(t) - q_j(t)) = \kappa(q_i^* - q_j^*), \forall (i,j) \in \mathcal{E}. \tag{6.69}$$

This completes the proof. □

6.6 Simulation results

In this section, we present simulation results to validate the effectiveness of the theoretical results. Consider a generic configuration in $\mathbb{R}^2$, given by

$$q^* = \begin{bmatrix} 0 & -0.8 & -2 & -2 & -1 \\ 0 & 1.6 & 2 & -2 & -2 \end{bmatrix}.$$

With q^*, the prescribed formation shape is depicted in Fig. 6.3. One universally rigid tensegrity framework associated with the configuration q^* is shown in Fig. 6.4, in which the dashed and solid lines represent the cables and struts, respectively.

Correspondingly, the stress matrix has the form

$$\Omega = \begin{bmatrix} 27.5 & -45 & 26.75 & -8.25 & -1 \\ -45 & 75 & -45 & 15 & 0 \\ 26.75 & -45 & 27.1250 & -9.375 & 0.5 \\ -8.25 & 15 & -9.3750 & 4.125 & -1.5 \\ -1 & 0 & 0.5 & -1.5 & 2 \end{bmatrix}.$$

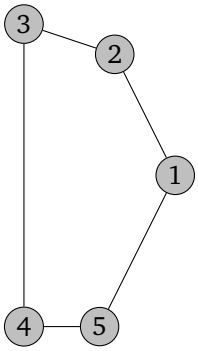

Figure 6.3: *Prescribed formation shape.*

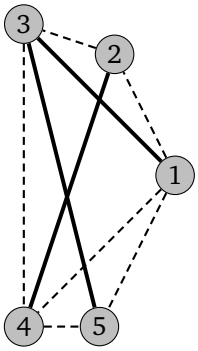

Figure 6.4: *Universally rigid tensegrity framework.*

The initial positions for the five agents are randomly chosen as

$$q(0) = \begin{bmatrix} -0.0573 & -1.4483 & -2.053 & -2.3178 & -1.6165 \\ -0.9285 & 2.0435 & 1.3054 & -1.7852 & -1.5231 \end{bmatrix}.$$

6.6.1 Formation scaling control using the proposed control law (6.3)

First, we consider the formation scaling control using only the stress. Let the formation scaling parameter κ be

$$\kappa = \begin{cases} 6, & 0 \leqslant t < 6, \\ 12, & 6 \leqslant t \leqslant 12. \end{cases}$$

To implement the control law(6.3), 2 pairs of nodes, $(1, 2)$ and $(2, 3)$, are chosen to constitute $\mathcal{V}_l$, and consequently $\mathcal{E}_l = \{(, 2), (2, 3)\}$, both of which are marked in blue in Fig. 6.5. To clearly show the variations of the formation shape at different time instants, we design an extra input, $u_e = [18, 0]^T$ for each agent. Since the extra input is constant and the same for each agent, it will not affect the stability of the closed-loop system. Then under the control law (6.3), the formation shapes at $t \in \{0, 2, 4, 6, 8, 10, 12\}$s are sequentially shown in Fig. 6.6, where the initial formation shape is zoomed in on the top. It can be seen that the desired formations with prescribed sizes are achieved for a piecewise constant scaling parameter κ. Fig. 6.7 shows that the scaling length errors, i.e., $\kappa\|q_i^* - q_j^*\| - \|q_i - q_j\|$, where the errors of the cables are plotted in the upper part and struts in the lower part. We can observe from Fig. 6.7 that all the edge lengths converge to their desired ones.

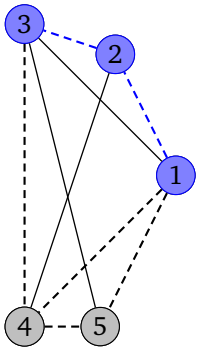

Figure 6.5: *The universally rigid framework with* $\mathcal{V}_l = \{1, 2, 3\}$ *and* $\mathcal{E}_l = \{(1, 2), (2, 3)\}$.

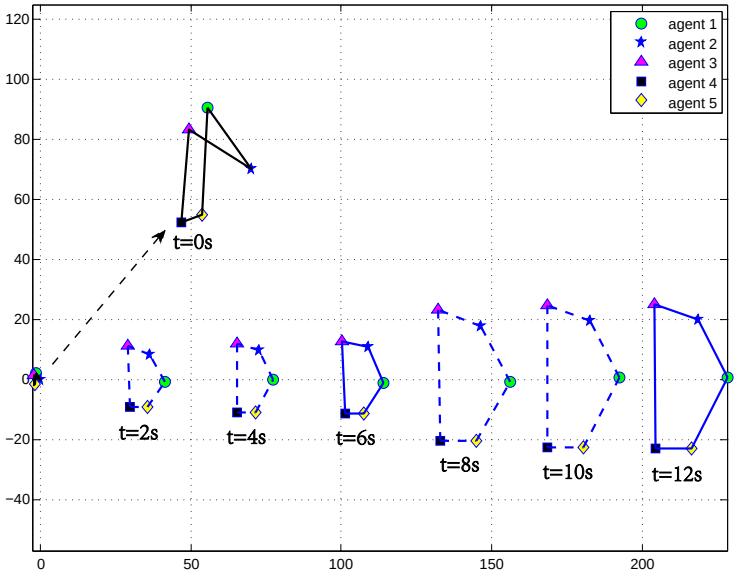

Figure 6.6: *Formation evolution using the control law* (6.3).

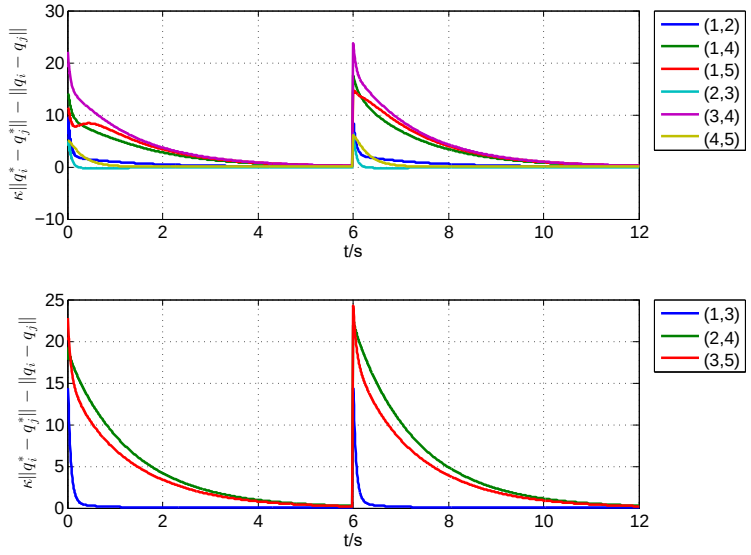

Figure 6.7: *Scaling length errors using the control law* (6.3).

6.6.2 Formation scaling control using the proposed control law (6.28)-(6.30)

We then consider the formation scaling control using the stress and the orthogonal projections. In this case, the formation scaling parameter is defined by

$$\kappa = \begin{cases} 6, & 0 \leqslant t < 6, \\ 12, & 6 \leqslant t < 12, \\ 6, & 12 \leqslant t < 18. \end{cases}$$

According to the principle of choosing $d+1$ pairs of nodes illustrated in Section 6.4, let $\mathcal{E}_l = \{(1,2),(2,3),(1,3)\}$ and $\mathcal{V}_l = \{1,2,3\}$, shown in Fig. 6.8. Following the formation scaling control laws (6.28)-(6.30) and the extra input $[18,0]^T$, the formation changes are sequentially shown in Fig. 6.9, in which the initial formation shape is again zoomed in on the top. It can be seen from Fig. 6.9 that the formation expands from $t = 0$s to 12s, and then shrinks until $t = 18$s, which agrees with the setup of the formation scaling parameter κ. The scaling length errors of cables and struts are presented in the upper and lower part of Fig. 6.10, which clearly shows the convergence of the lengths of all edges to the desired ones.

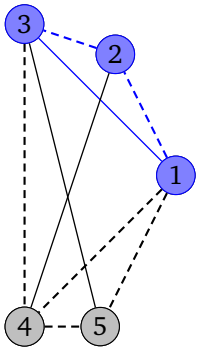

Figure 6.8: *The universally rigid framework with* $\mathcal{E}_l = \{(1,2),(2,3),(3,1)\}$.

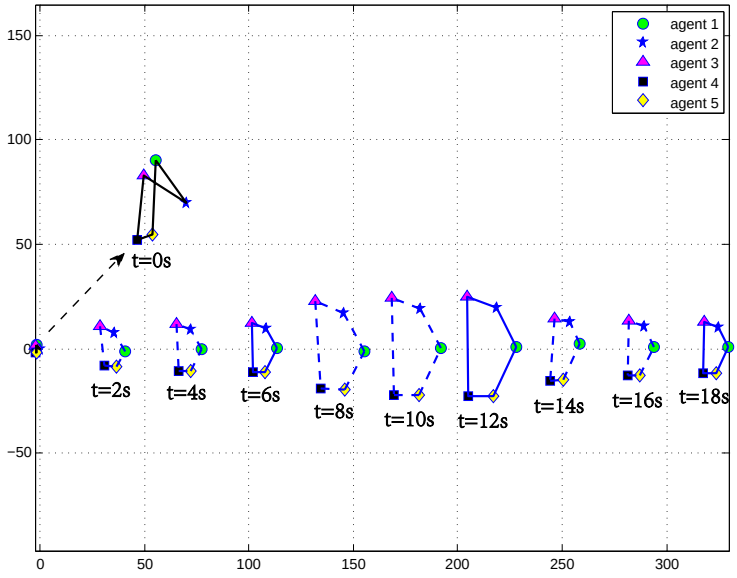

Figure 6.9: *Formation evolution using the control laws* (6.28)-(6.30).

6.6.3 Formation scaling control using the proposed control law (6.52)-(6.53)

In this subsection, we present the numerical simulation results of the proposed estimation-based controller (6.52)-(6.53). The scaling parameter κ is set to be a constant scalar 10 at all times. The subgraph $\mathcal{G}(\mathcal{V}_l, \mathcal{E}_l)$ is constructed the same as Fig. 6.5, in which only agent 1 knows the precise information of κ, while agents 2 and 3 approach the scaling information by estimation. Again, to separate the

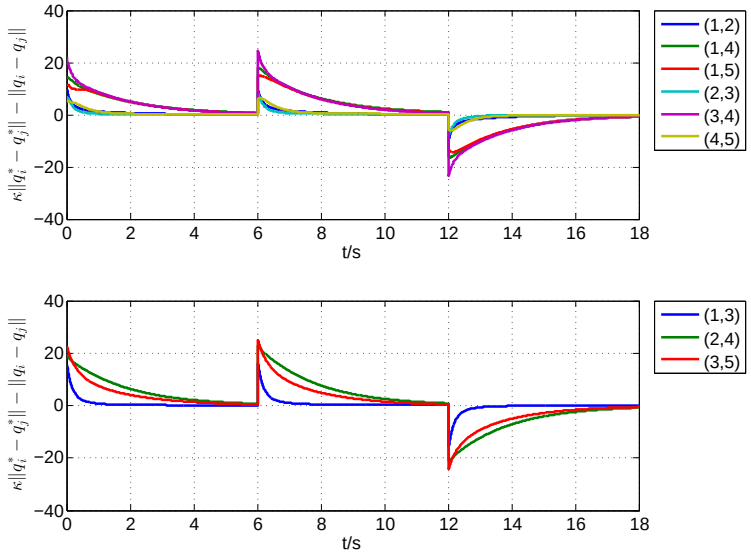

Figure 6.10: *Scaling length errors using the control laws* (6.28)-(6.30).

formation patterns at different time instants, we design an additional input $[2.5, 0]^T$ accompanying the control law (6.52)-(6.53). From Fig. 6.11, we can see that the formation shape starts from an anomalous status and finally converge to the desired shape. The corresponding scaling length errors are shown in Fig. 6.12, where the errors of cables and struts are presented in the upper and lower part, respectively. It is clear that the errors of all the members converge to zero.

6.7 Concluding remarks

In this chapter, we have addressed the formation scaling problem for multi-agent systems. First, by employing the stress of universally rigid tensegrity frameworks, we have designed distributed control laws to achieve the formation shape with the prescribed size. Then to relax the constraint that the formation scaling parameter has to be known to d pairs of agents in $\mathbb{R}^d$, we have proposed a class of new distributed control laws that utilize the (orthogonal) projections. It has been shown that the desired formation scaling can be achieved under the mild assumption that only one pair of agents knows their desired relative positions. Moreover, we have constructed a relative-position-based estimator to further reduce the number of agents knowing the scaling parameter, so that only one agent is informed of the scaling size of the formation. Relying on the estimator, all the agents can be driven to form the desired formation under the proposed control laws.

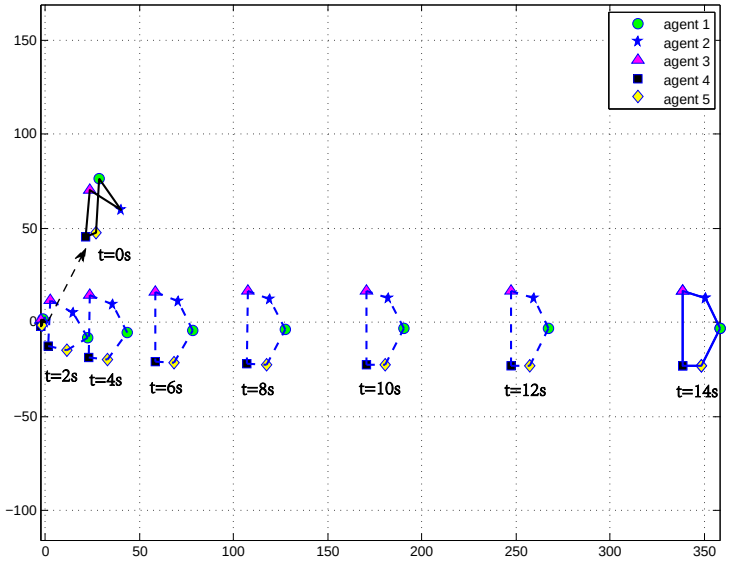

Figure 6.11: *Formation evolution using the control laws* (6.28)-(6.30).

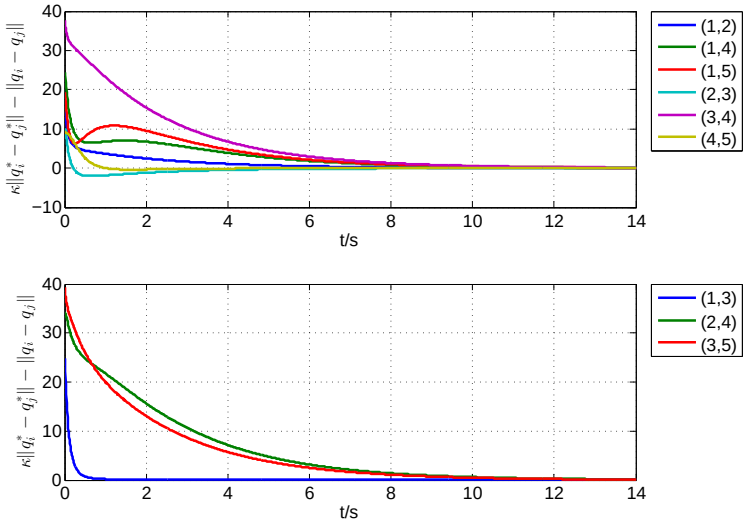

Figure 6.12: *Scaling length errors using the control laws* (6.28)-(6.30).